On the Crystallization of Compacted and Chunky Graphite from Liquid Multicomponent Iron-Carbon-Silicon-Based Melts

D.M. STEFANESCU, R. HUFF, G. ALONSO, P. LARRAÑAGA, E. DE LA FUENTE, and R. SUAREZ

Extensive SEM work was carried out on deep-etched specimens to reveal the evolution of compacted and chunky graphite in magnesium-modified multicomponent Fe-C-Si alloys during early solidification and at room temperature. The findings of this research were then integrated in the current body of knowledge to produce an understanding of the crystallization of compacted and chunky graphite. It was confirmed that growth from the liquid for both compacted and chunky graphite occurs radially from a nucleus, as foliated crystals and dendrites. The basic building blocks of the graphite aggregates are hexagonal faceted graphite platelets with nanometer height and micrometer width. Thickening of the platelets occurs through growth of additional graphene layers nucleated at the ledges of the graphite prism. Additional thickening resulting in complete joining of the platelets may occur from the recrystallization of the amorphous carbon that has diffused from the liquid through the austenite, once the graphite aggregate is enveloped in austenite. With increasing magnesium levels, the foliated graphite platelets progressively aggregate along the c-axis forming clusters. The clusters that have random orientation, eventually produce blocky graphite, as the spaces between the parallel platelets disappear. This is typical for compacted graphite irons and tadpole graphite. The chunky graphite aggregates investigated are conical sectors of graphite platelets stacked along the c-axis. The foliated dendrites that originally develop radially from a common nucleus may aggregate along the c-axis forming blocky graphite that sometimes exhibits helical growth. The large number of defects (cavities) observed in all graphite aggregates supports the mechanism of graphite growth as foliated crystals and dendrites.

I. INTRODUCTION

MULTICOMPONENT Fe-C-Si-Mn-S-*etc.* alloys, known in industry as cast irons, solidify with a stable austenite/graphite (γ/Gr), or metastable γ/Fe$_3$C eutectic. The stable form of the carbon-rich phase, the graphite, crystallizes from the liquid with a variety of morphologies, depending on the chemical composition and the solidification conditions (cooling rate). The main morphologies include lamellar (LG), compacted or vermicular (CG), and spheroidal (SG) graphite. Other "degenerated" or intermediate forms include, but are not limited to, chunky and exploded graphite. An LG-to-CG-to-SG transition can be triggered through the addition of small amounts of Mg, Ce, or lanthanides to a low sulfur iron. The process is reversible: SG will revert to LG with sulfur addition or through loss of magnesium by evaporation and/or oxidation. The CG-to-LG transition is sensitive to the specific elements used to produce it. It was found that the transition from compacted to lamellar shape was continuous for Mg treatment, whereas a sharp transition was found when lanthanides were used for graphite shape modification.[1]

This work is concerned with the crystallization of compacted and chunky (CHG) graphite. Typical examples of these morphologies are presented in Figure 1 after Reference 2 and 3. It is seen that both forms of graphite are highly interconnected and appear to grow radially outward.

Earlier SEM investigation conducted on deep-etched Fe-C-Si samples of industrial composition, obtained through interrupted solidification, revealed the sequence of evolution of graphite aggregates morphology as the amount of magnesium in the composition increases. It was demonstrated that when the residual magnesium increases from <0.01 to 0.22 pct, graphite morphology evolves from the lamellar type, to curly graphite, to tadpole graphite, and then to mixtures of compacted, chunky, and imperfect spheroidal graphite. The less common graphite morphologies, curly and tadpole graphite, are presented in Figure 2. The tadpole graphite

D.M. STEFANESCU, Professor Emeritus, is with The Ohio State University, Columbus, OH, and also with The University of Alabama, Tuscaloosa, AL. Contact e-mail: stefanescu.1@osu.edu R. HUFF, Technical Team Leader, is with Manufacturing Technology, PD&GT, Caterpillar, Peoria, IL. G. ALONSO and P. LARRAÑAGA, Project Leaders, and E. DE LA FUENTE, Junior Researcher, are with the Área Ingeniería, I+D y Procesos Metalúrgicos, IK4-Azterlan, Durango, Spain. R. SUAREZ, Manager R&D of Metallurgical Processes, is with the Veigalan Estudio 2010, Durango, Bizkaia, Spain.

(TPG) is a graphite spheroid that has developed one or more tails.[4] The graphite spheroids are surrounded by austenite early in the solidification process, while tadpole graphite was in most cases connected to cementite, suggesting growth in contact with the liquid. It behooves now to explain the mechanism of these transitions.

Growth of lamellar graphite is fairly well understood, but that of compacted, chunky, and spheroidal graphite is still the focus of research. The highly three-dimensional (3-D) branched morphology of CG was revealed as early as 1979 through successive polishing and reconstruction of the two-dimensional (2-D) microstructure,[6] and then confirmed through deep etching and graphite extraction (Figure 1(a)), and through focused ion beam nano-tomography.[7] An early model derived from SEM analysis of deep-etched metallographic samples[8] suggests that while the lamellar graphite/austenite eutectic grain grows in a radial manner with graphite lamellae made of graphite sheets that bend, twist, and branch, while growing in the a-direction, a reorientation of the graphite sheets occurs when transiting to CG. This reorientation gives the appearance of growth along the c-axis. As growth proceeds, the contact with the liquid is lost, and the tip of CG may develop conical sectors. In a similar model,[9] the transition from LG to CG or from SG to CG is also based on changing of the growth direction of the graphite aggregate from the a- to c-direction, or from c- to a-direction.

Chunky graphite, a highly branched, interconnected form of graphite, is a degenerated form of spheroidal graphite reported as early as 1970.[10] It has the same radial structure as spheroidal graphite with dominant growth occurring along the c-axis of the graphite crystal. Liu et al.[11] proposed a growth model in which chunky graphite is characterized by a series of clustered, sector-shaped graphite segments.

All three models discussed in this section postulate growth of the graphite crystal along the c-direction for CG and CHG. SEM and TEM observations confirm the existence of conical sectors made of parallel graphite planes, as shown in the figures associated with the models. Yet, significant growth of the graphite crystal along the c-axis is highly improbable, and not supported by direct experimental observations.

A possible explanation for the development of graphite aggregates in the c-direction is the growth as foliated crystals or dendrites.[12,13] Foliated dendrites (Figure 3) are assemblies of thin plates connected with thin protrusions growing perpendicular to the basal planes, and separated by solvent impurity layers. They have been identified by Saratovkin[14] as early as 1959 when he studied the growth of hexagonal platelets of cadmium iodide crystals, and then used the foliated dendrite growth mechanism to explain iron entrapment between graphite layers during graphite growth in cast iron.

The morphology of graphite in Fe-C-Si alloys is the result of a four-stage growth process: (1) in the liquid, (2) in the liquid during the eutectic solidification, (3) during cooling to the eutectoid temperature, and (4) during the eutectoid transformation. However, in this paper, we will mostly be concerned with graphite growth in contact with the liquid. The goal of this work is to further document that indeed graphite growth of
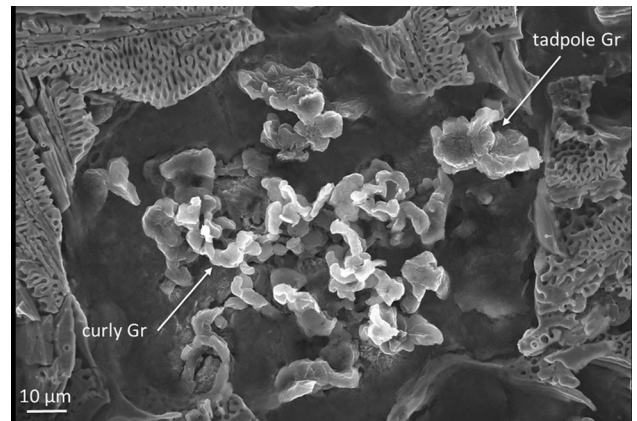

Fig. 2—SEM deep-etched micrograph of an iron with 0.013 pct Mg: curly and tadpole graphite.[5]
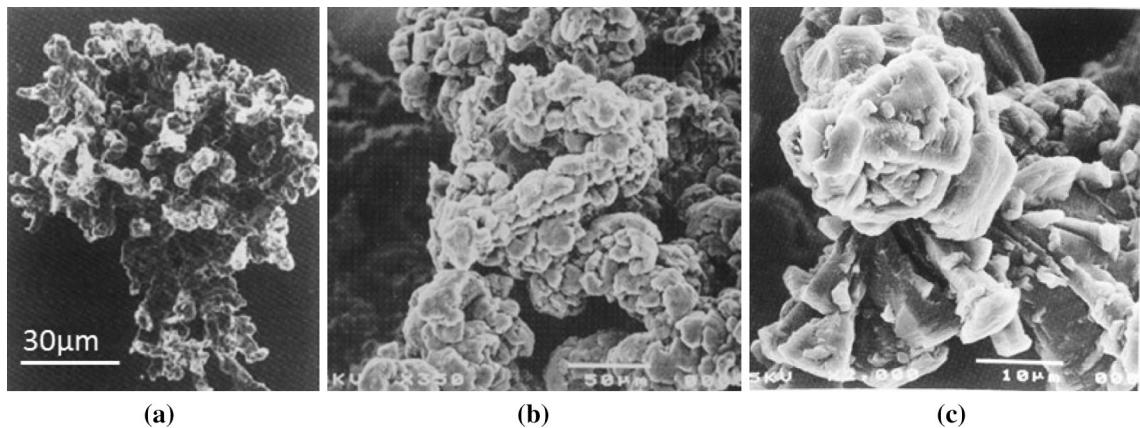

Fig. 1—Typical graphite shapes obtained from commercial cast iron through deep etching and extraction: (a) compacted graphite[2]; (b) chunky graphite[3]; (c) higher magnification of chunky graphite in (b).[3]
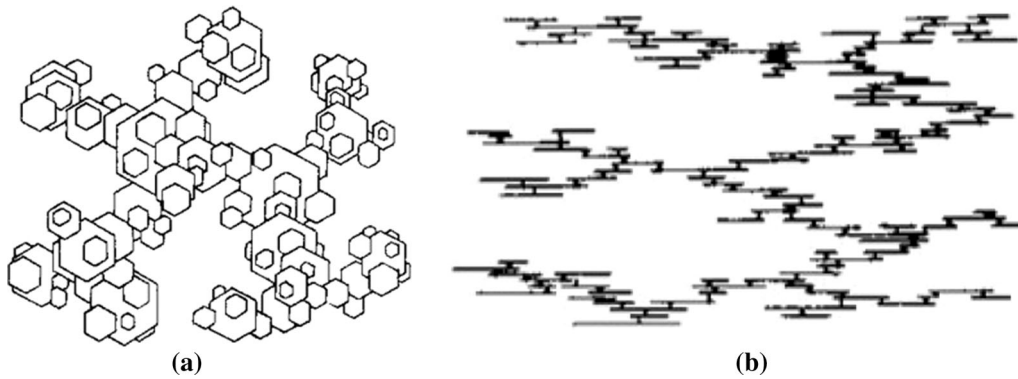
(a)   **(b)**

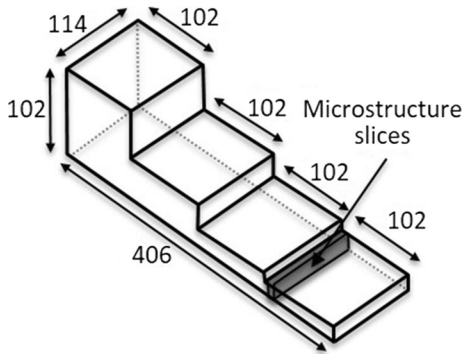Fig. 3—A foliated dendrite[14]: (a) top view; (b) side view.

Fig. 4—Drawing of the cast specimen and region where the metallographic sample was extracted for melt CG-S-Sb; the thickness of the plates was 102, 51, 25, 16 from left to right (dimensions in mm).

compacted and chunky graphite occurs through the foliated dendrite mechanism.

II. RESEARCH APPROACH AND RESULTS

The material for in-depth SEM analysis of graphite morphology was obtained from two laboratory Fe-C-Si melts of commercial purity with the composition designed to produce compacted graphite (CG-Q5 and CG-S-Sb), and from two industrial melts designed to produce compacted (CG-S) and spheroidal and chunky (CHG-S) graphite. Antimony was used in melt CG-S-Sb as it is known to have an adverse effect on graphite compaction. Melt CHG-S exhibited a significant amount of chunky graphite. All melts were treated with Mg-containing ferrosilicon alloys to modify the graphite shape, and then post-inoculated in the pouring ladle with standard foundry inoculants.

From melt CG-Q5, six standard thermal analysis cups (36 × 36 × 43 mm) were poured. The solidification of the cups was interrupted by quenching in brine (to increase the thermal conductivity) at increasing times, to provide information on the microstructure at various stages during solidification. Detailed description of the procedure for the preparation of melt CG-Q5 was given elsewhere.[5,13]

CHG-S was obtained from the center of a sand-cast cube 300 mm long on each side, from an iron studied in previous work.[15] CG-S was extracted from a 12-mm-thick area of an industrial sand casting that fulfills the requirements of the grade EN-GJV-300 according to UNE-EN 16079.

The metallographic specimen from melt CG-S-Sb was obtained from a sand-cast step block near the fracture surface of a tensile bar machined from the region showed in Figure 4.

To reveal the morphology of the graphite, the metallographic samples were deep etched to remove the matrix, as described in detail in a previous publication.[5] The deep-etched samples were then examined with an Ultra PLUS Carl Zeiss SMT with 0.8 nm resolution at 30 kV in the STEM mode. An X-Max 20 Oxford Instruments EDS detector with a resolution of 127 eV/mm^2 was used to determine the local chemistry of graphite nuclei.

The chemical composition of all samples and the room-temperature overall graphite morphology is given in Table I. The CG-Q5 iron contained 0.04 pctCr, 0.01 pctMo, 0.04 pctNi, 0.04 pctCu, and less than 0.01 pctAl, in addition to the elements listed in the table. The Mg and S contents of melt CG-S are unusually low for an industrial iron.

The interrupted solidification experiments with the compacted graphite iron from series CG-Q5 provided an insight in the evolution of graphite morphology during early solidification. The microstructure consisted of a mixture of SG, TPG, CG, and even some CHG. The SEM micrographs of a tadpole graphite shown in Figure 5 demonstrate that both the tail and the quasi-spheroidal region of the TPG are made of graphite platelets with local orientation but highly disorganized orientation at a larger scale. It is further noticed that the parallel platelets are not in contact with one another on their entire surface, but exhibit clear separation along the {0001} planes. This distribution of the platelets is consistent with the concept of foliated crystals.

Foliated graphite platelets are also found in the few chunky graphite formations found in the quenched sample. A clear example of such a platelet is shown in Figure 6. The chunky graphite appears to be built of foliated platelets stacked along the c-direction.

Table I. Chemical Composition (Mass Pct) of Experimental Cast Irons

Melt	CE	C	Si	Mn	P	S	Mg	Sb	Sn	Others
CG-Q5	4.32	3.68	2.14	0.14	0.016	0.014	0.020	trace	trace	0.021Ti
CG-S	4.44	3.74	2.26	0.28	0.028	0.001	0.008	trace	trace	<0.005Ce
CG-S-Sb	4.35	3.70	2.11	0.34	0.017	0.012	0.013	0.01	0.09	0.16Cu, 0.2V, 0.014Ce
CHG-S	4.38	3.72	2.09	0.12	0.033	0.012	0.052	0.002	0.005	0.006La

SG spheroidal graphite, *CG* compacted graphite.
CE Carbon equivalent calculated as pctC + 0.31·pctSi + 0.33·pctP−0.027·pctMn + 0.4·pctS.
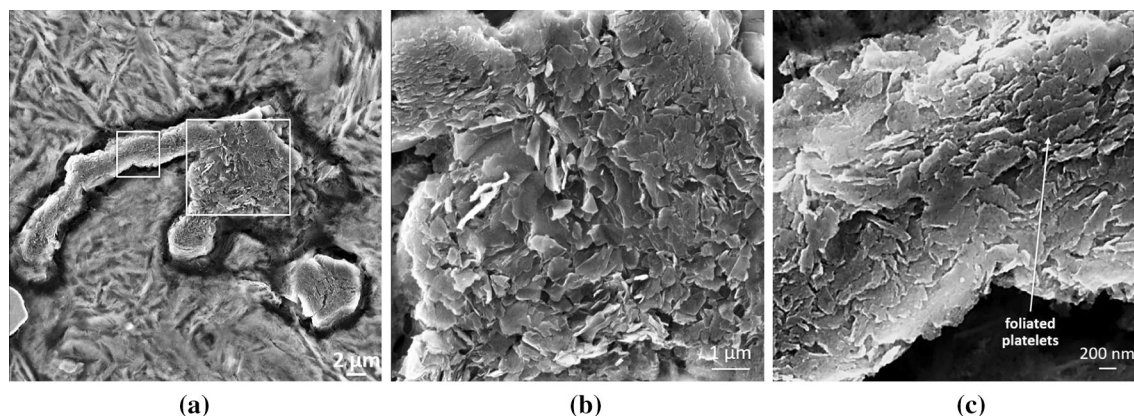

Fig. 5—SEM deep-etched micrographs of a tadpole (melt CG-Q5): disorganized growth of foliated graphite platelets[4]: (*a*) tadpole graphite; (*b*) higher magnification of region in (a); (*c*) higher magnification of region in (a).
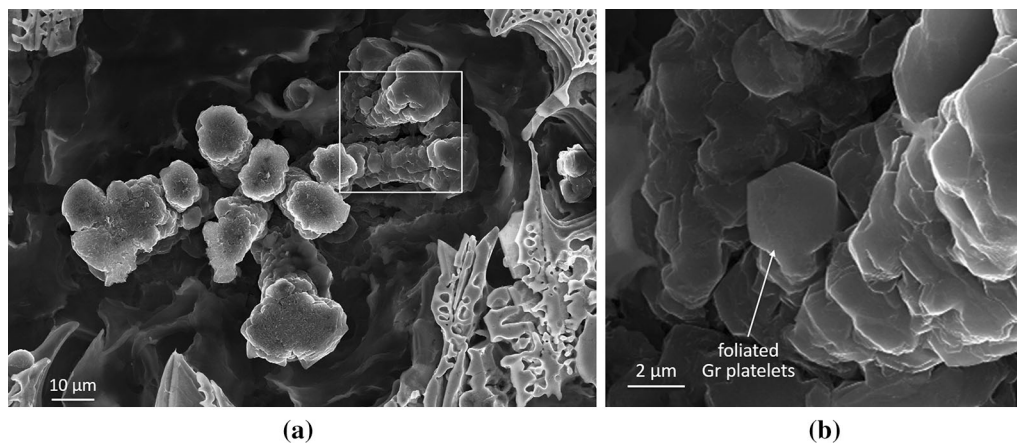

Fig. 6—SEM deep-etched micrographs of chunky graphite from melt CG-Q5 at two magnifications (the lower magnification on the left is reprinted from Ref. [13]: stacking of foliated graphite platelets in the *c*-direction).

Previous work[4] has demonstrated that compacted graphite is also made of stacked platelets, but the foliated nature of these platelets was not obvious. Additional images of stacked foliated graphite platelets in compacted graphite from a sample cooled to room temperature are provided in Figure 7. Note the rough interface of the compacted graphite aggregate.

The best examples of foliated dendrite in CG iron were obtained in the antimony-containing melt CG-S-Sb. A general microstructure is shown in Figure 8. The dendritic nature of the graphite aggregate is clearly seen. One of the extremities of the largest graphite

aggregate has the appearance of chunky graphite. In an attempt at explaining the unusual growth pattern, EDS analysis was conducted along a line crossing the apparent center of the graphite aggregate (Figure 9). Antimony, which was originally believed to be the main reason for this structure was found in the nucleus but not in the graphite or in the matrix. Vanadium, Sn, and Ce were found in the graphite, but not in the nucleus.

Additional details of the graphite morphology from the same sample are provided in Figure 10. The stacking of the foliated hexagonal faceted graphite platelets is seen throughout. In addition, defects looking as black
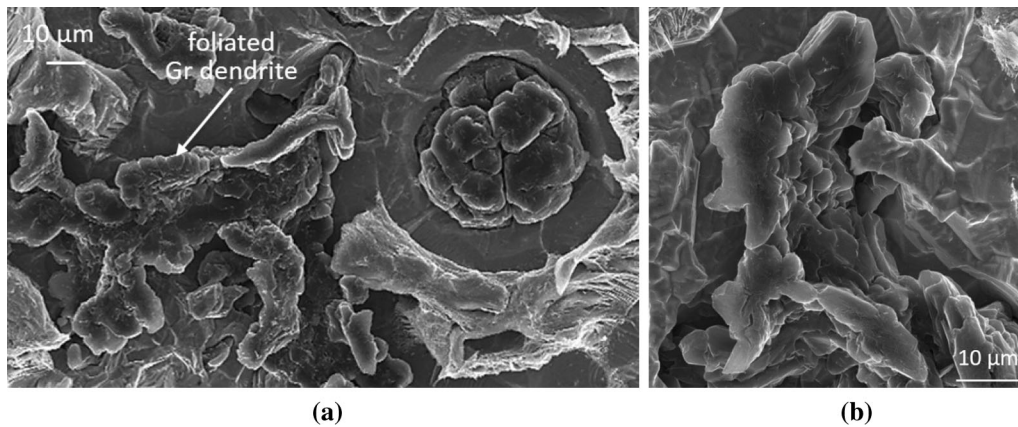
(a)   **(b)**

Fig. 7—SEM deep-etched micrograph of sand-cast sample from melt CG-S: (*a*) foliated platelets on CG and conical sectors in an imperfect graphite spheroid; (*b*) stacking of graphite platelets on CG.
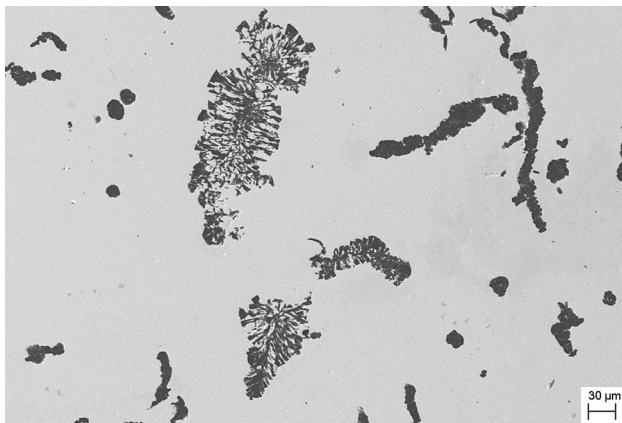

Fig. 8—Optical unetched micrograph of sand-cast sample from melt CG-S-Sb: dendritic growth of graphite.

voids appear on the originally polished surface of the graphite aggregate (Figure 10(a)). These defects are consistent with the growth of foliated dendrites, as the iron can be incorporated between the dendrite arms (graphite platelets) during solidification. This particular feature is illustrated in Figure 10(b), where the well-formed hexagonal platelets are well separated from one another with a tiled-roof configuration. A spiral dislocation growth is also seen on the higher magnification micrograph. In a different region of the sample, the graphite platelets have morphed into graphite clusters with the apparent growth in the *c*-direction, producing blocky graphite (Figure 10(c)). The hexagonal configuration of the graphite platelets is less distinct.

A general microstructure of a chunky graphite region is presented in Figure 11. The chunky graphite appears in round patches that extend into the interdendritic regions. The interconnected structure of the chunky graphite has been documented by various investigators[3,11,16] and is also visible in Figure 6. A closer examination reveals that foliated platelets are growing in the *a*-direction in both length and width, and then appear to rotate around the *c*-axis (Figure 12(a)) in a process that could be considered to be helical growth, as

advocated by Double and Hellawell.[17,19] The foliated dendritic growth of this type of graphite is further documented in Figure 12(b). In this instance, the foliated graphite platelets grow parallel but separated from one another, and have lost almost completely their hexagonal shape.

III. DISCUSSION

It is generally accepted that the growth of graphite in cast iron starts with the formation of two-dimensional (2-D) one-atom-thick layers of crystalline graphite (graphene sheets). The graphene layers can stack into two types of structural units, carbon nano-rods (cluster of 8-10 graphene layers with diameters of about 2.5 nm and lengths of 15-100 nm) or carbon nano-platelets (sets of 5-25 graphene stacks with 2.5 nm thickness and 10×32 nm surfaces).[18]

The graphene sheets can grow easily in the $\langle 10\bar{1}0 \rangle$ direction (*a*-direction) of the hexagonal crystal lattice of graphite, to produce a multilayer sheet (graphite lamella or plate). A hypothesis that attempts to explain thickening of the graphite plate through growth in the *c*-direction is that growth in the *a*-directions is partially inhibited when surface-active impurities (S, O, N) are adsorbed at the unsaturated edges of a graphene platelet.[19] Thus, growth in the $\langle 0001 \rangle$ direction (*c*-direction) becomes more probable. As lamellar graphite iron melts are relatively rich in O and S, the 3-dimensional (3-D) graphite plates grow in the crystallographic *a*-directions with the {0001} basal planes parallel to the plane of the lamellae, and thicken in the *c*-direction.

The body of evidence presented in this and previous work[4,12,13,18,19] leads to the conclusion that graphite growth in multicomponent Fe-C alloys starts with graphene sheets that develop into hexagonal faceted graphite platelets of micron-size dimension (nanometer height in the *c*-direction and micrometer width in the *a*-direction), which are the building blocks of all graphite morphologies encountered in cast iron. Double and Hellawell[20] may have inferred to the existence of such building blocks when they stated that graphite lamellae
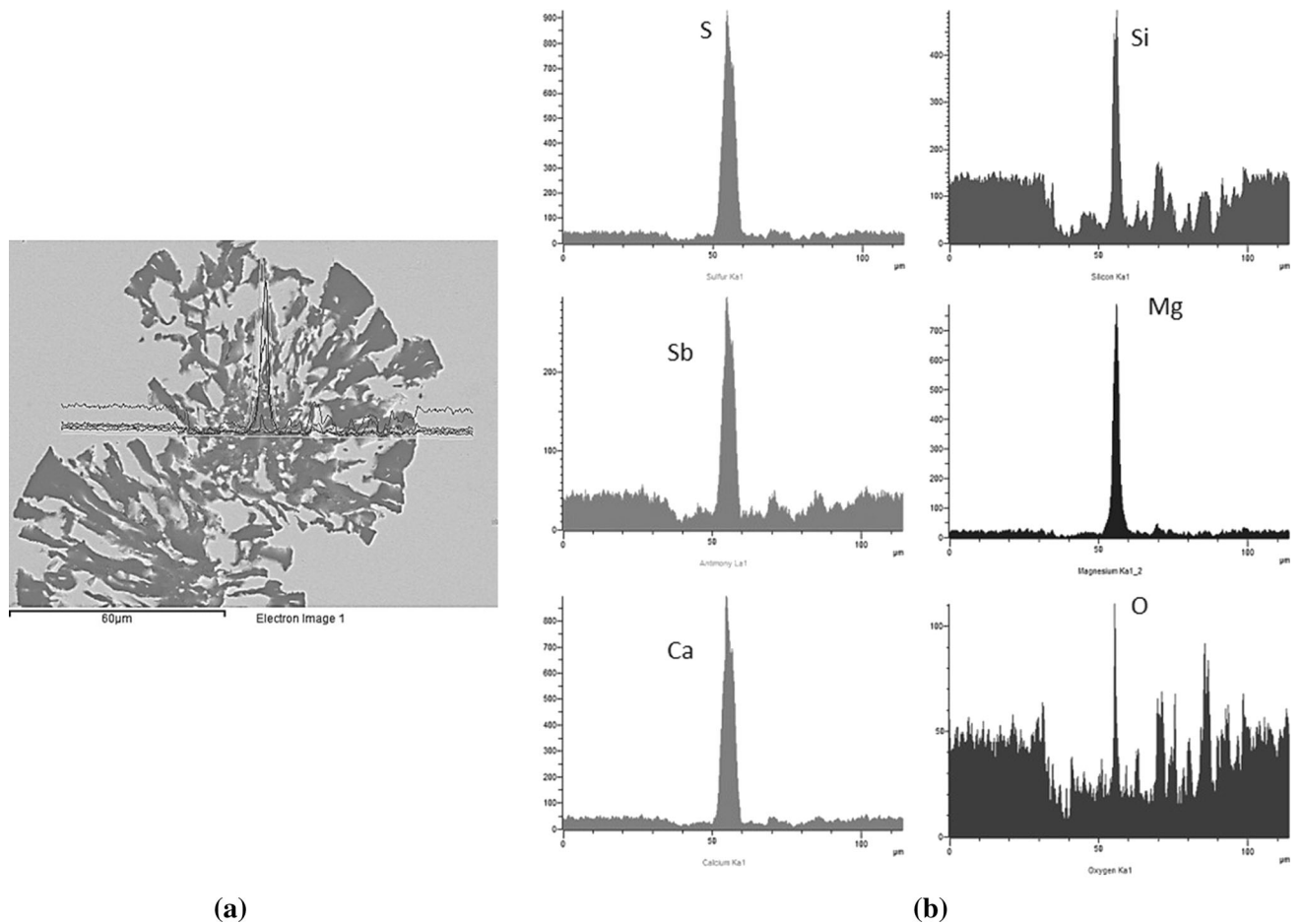
(a)

(b)

Fig. 9—Chemical composition (EDS) along a line through the center of a graphite dendrite from melt CG-S-Sb: nucleus made of complex Ca, Sb sulfide, and probably Mg silicate.

are composed of layers of fault-free crystal some 10^{-4} mm thick. The platelets grow to form the foliated dendrites,[13] and sometimes, classic stem dendrites.

Foliated dendrite growth was observed in other metallic alloys such as an Al-Ti alloy, where the faceted Al_3Ti phase developed into "tiled-roof" structure.[21] The growth of protuberances to produce foliated dendrites was also observed (Figure 13).

Since large kinetic limitation to growth of the facets is typical for faceted crystals such as graphite, high constitutional undercooling is required to break down the planar interface.[22] Thus, in the absence of significant constitutional undercooling, the graphite aggregate will grow as large plates (lamellae in 2-D) made of hexagonal faceted platelets distributed in a tiled-roof configuration, as described in previous work.[13] The graphite aggregates grow from the center in radial dendritic manner, in the general *a*-direction of the platelets. The plates develop twins[23] and branch as they grow. Such twins were noted in recent TEM work on a graphite lamella.[24]

Because of the asymmetric shape of the Fe-C equilibrium phase diagram, solidification of austenite is expected to occur even in irons of eutectic composition. As magnesium has extremely low solubility in solid iron, the solid/liquid partition coefficient is very small and Mg is strongly rejected in the liquid at the tip of the graphite platelets that grow in the *a*-direction, increasing the constitutional undercooling. Solute accumulates preponderantly on the {0001} faces of the graphite crystal where growth rate is retarded. Spiral growth around a screw dislocation emerging at the center of the platelet face will produce a protuberance. When the protuberance penetrates the layer of accumulated solute, the anisotropy of the crystal will become again the dominant effect on its growth, and parallel growth to the initial platelet will occur producing a new platelet (Figure 14(a)). With increased undercooling, several protuberances may develop on the (0001) faces of the platelets as shown in Figure 14(b), producing increased branching of the foliated dendrites.

Other elements that have a low partition coefficient, such as Bi, Pb, and Sb, will also promote higher constitutional undercooling. The growth of the graphite platelets becomes more intricate, as foliated crystals and dendrites start meandering in three dimensions. As constitutional undercooling increases because of higher cooling rate or solute accumulation at the liquid/graphite interface, branching of the dendrites increases. The graphite platelets grow in many different directions (Figure 5), and their hexagonal shape becomes less regular.
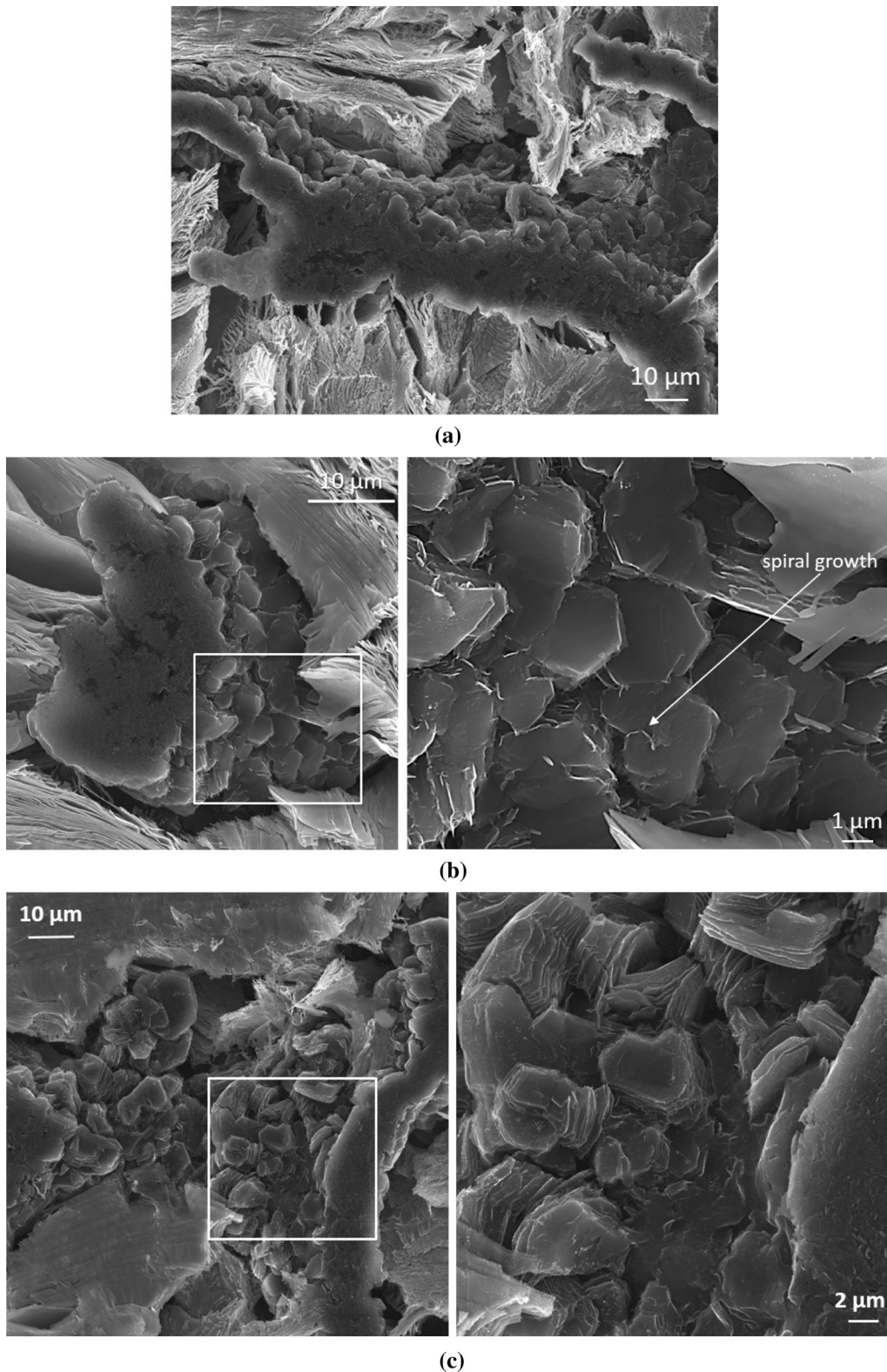
Fig. 10—SEM images of deep-etched sand-cast samples from melt CG-S-Sb: foliated graphite dendrites. (*a*) Foliated growth of graphite platelets; (*b*) foliated dendritic growth of graphite platelets at two magnifications; (*c*) formation of graphite clusters (blocky graphite) from the foliated platelets at two magnifications.

Curved platelets were also observed in compacted and chunky graphite aggregates. It was shown that oxygen may cause bending of the graphene layers.[25] It is probable that Mg has a similar effect. Clusters of platelets with different orientation appear, although the overall aspect is still, in many cases, that of foliated

dendrites. The overall graphite aggregate is thicker in the *c*-direction compared with the lamellar graphite aggregate.

The high-resolution SEM micrograph of a compacted graphite aggregate in Figure 15 shows clusters of parallel hexagonal platelets with no rotational faults. The clusters assume different general orientation. In many instances, the separation between the platelets within the clusters disappears, with the formation of blocky graphite. Such "graphite blocks" were also identified by TEM.[26] Also some plates grow at a different angle than the ones on which they originate. The growth mechanism in this case can be neither two-dimensional, nor spiral dislocation nucleation. It is probably a dendrite branching mechanism, with new platelets branching out of old ones at screw dislocation defects.

Based on the comprehensive SEM analysis in this work, the growth mechanism for compacted graphite can be summarized through the graphic representation in Figure 16. The dendritic appearance and the foliated crystal growth are clearly visible. The graphite platelets growing in the *a*-direction form the stem of the dendrite. In the tip of the CG aggregate (right of figure), the platelets become highly disorganized, and eventually
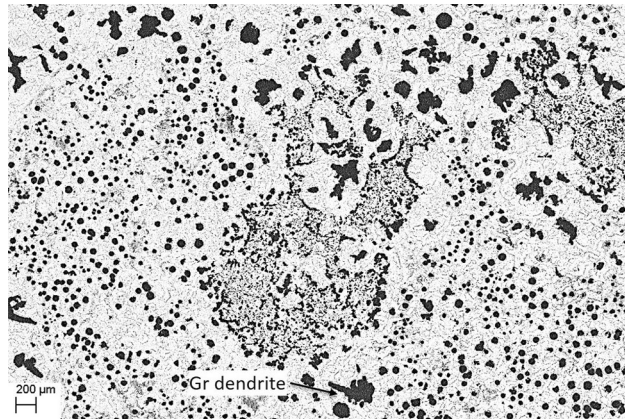
change their stacking preferentially along the *c*-axis of the graphite crystals. This gives the appearance of chunky graphite or even spheroids. This mechanism explains all three forms of graphite—compacted, chunky, and spheroidal.

Thickening of the platelets occurs through growth of additional graphene layers nucleated at the ledges of the graphite prism as shown in Figure 17. The graphite platelets in the figure appear to be separated in the *c*-direction, which is consistent with the growth of foliated crystals. The foliated growth mechanism resulting in stacking of the platelets does not require 2-D nucleation as suggested in recent work.[26,27]

At higher Mg levels, and therefore higher constitutional undercooling, the graphite morphology changes from compacted to chunky and spheroidal. The overall growth of the graphite aggregate remains radial. The chunky graphite aggregate exhibits dendritic growth of quasi-cylindrical sectors of graphite platelets stacked along the *c*-axis, growing radially from a common nucleus (see for example Figure 6 and Reference 28). The development of the graphite aggregate in the *c*-direction may occur through the foliated crystal mechanism producing conical sectors. Sometimes, the quasi-cylindrical sectors are made of stacks of blocky graphite, while in other instances, such as in
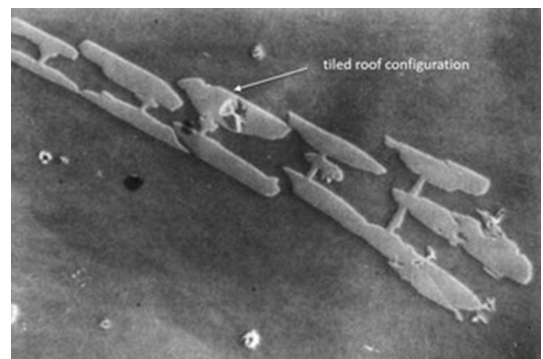

Fig. 11—Optical unetched micrograph of sand-cast sample from melt CHG-S: chunky and spheroidal graphite.

Fig. 13—Al₃Ti foliated dendrites with tiled-roof configuration in Al-1.15 wt pct Ti alloy; magnification 40 times.[21]

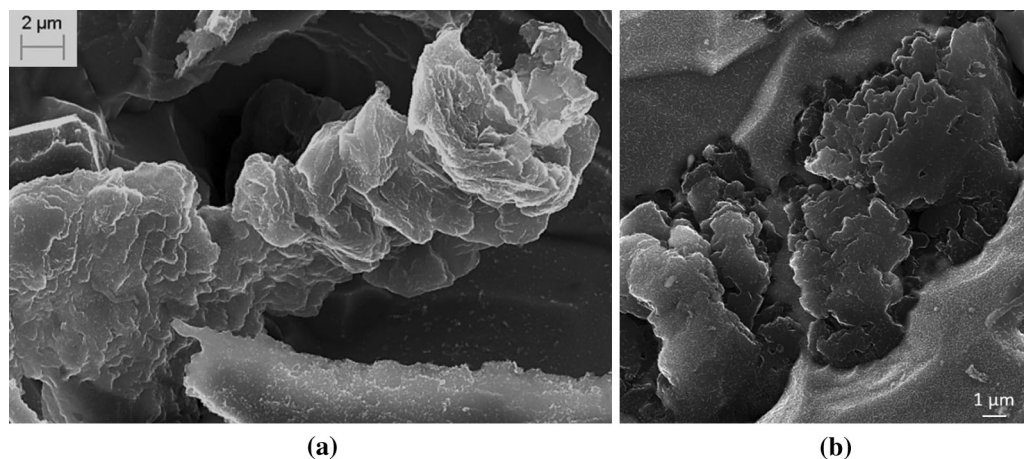(a)   (b)

Fig. 12—SEM images of deep-etched sand-cast samples from melt CHG-S: (*a*) chunky graphite aggregates; (*b*) foliated graphite platelets.
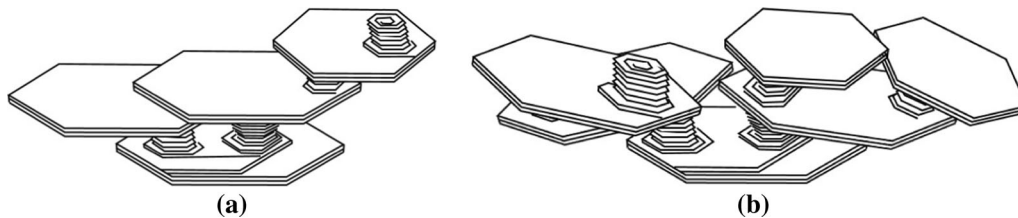
Fig. 14—Schematic representation of the growth mechanism of foliated dendrites: (*a*) growth of graphite platelets as foliated dendrite organized in a tiled-roof configuration; (*b*) growth of graphite platelets as disorganized foliated dendrite.
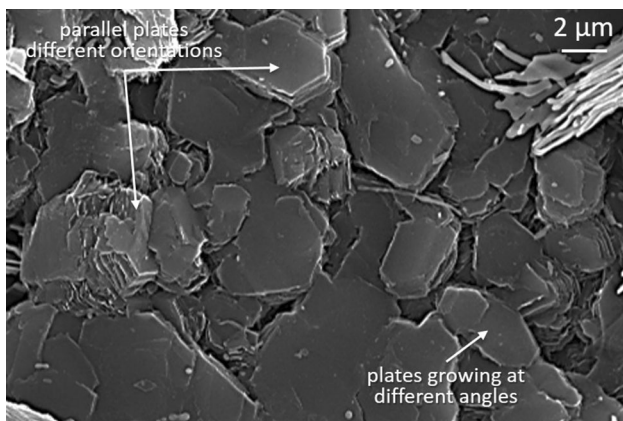

Fig. 15—High-resolution SEM of faceted platelets in a compacted graphite aggregate (melt CG-RT-Sb).
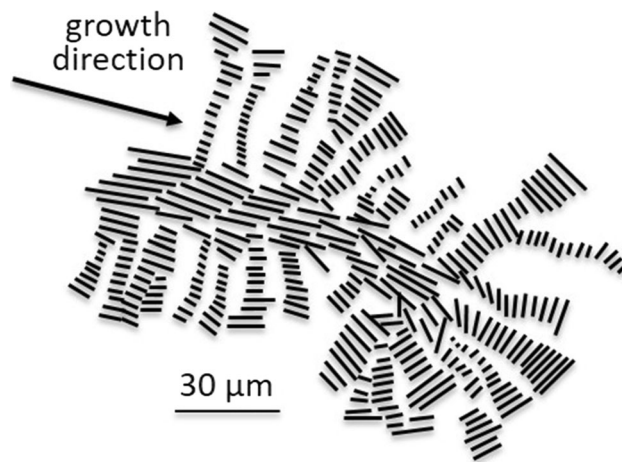

Fig. 16—Schematic representation of the growth mechanism of a compacted graphite aggregate.

Figure 12(a), foliated platelets grow in a helical mode. Most platelets have lost their clear hexagonal shape, as the {10$\bar{1}$0} faces become rougher. Examples of limited helical growth are found in both compacted and chunky graphite growth, as shown in Figure 18. However, complete conical helices, as postulated by Double and Hellawell, were not found. Chunky graphite can be the product of a succession of conical sectors growing on top of one another. It is not uncommon for CHG to exhibit a quasi-spherical shape at the tip (see for example Figure 18(b)), which led researchers to imply that this is a degenerated form of SG. We believe that the quasi-spherical tip develops once the direct contact with the liquid is lost. As such, it is the result of growth through carbon diffusion through the austenite shell.

While the object of this study did not include graphite spherulites, a few comments are necessary to situate this research in the larger context. A dendritic form of graphite on an imperfect graphite spherulite found in a Ni-C melt was reported as early as 1963.[29] Minkoff[30] then argued that pyramidal growth of graphite occurs because of morphological instability. The graphite extracted from Ni-C solutions appeared to be dendritic. Later, Hamasumi[31] identified graphite spheroids with protruding dendritic patterns in a large SG iron casting.

TEM evidence of circumferential growth of graphite spherulites has been found to exist in both spheroidal graphite in a Fe-C alloy[32] and for amorphous graphite growing in an electronic beam[33] (Figure 19). However, no evidence of curved crystal growth in the *a*-direction

as suggested by Sadocha and Gruzleski[34] was uncovered in this research. Thus, it is reasonable to conclude that such a growth mechanism is only possible after graphite encapsulation in an austenite shell, when further graphite growth occurs through carbon diffusion from the melt to the graphite through the shell. The amorphous graphite deposited on the existing graphite is then recrystallizing and produces curved graphite layers as Figure 19 suggests. Recrystallization is also most likely a mechanism through which the graphite platelets, initially separated are joined during growth of the graphite aggregate through the austenitic shell.

A schematic summary of the growth mechanism of lamellar, compacted, and chunky graphite is presented in Figure 20. At first glance they may not look too much different from the earlier drawings in References 6, 9 and 11. Yet the difference is fundamental. The proposed mechanism emphasizes that all graphite aggregates are made of graphite platelets, which are the building blocks, growing from a nucleus. The graphite crystals (platelet) grow in the *a*-direction, with limited thickening in the *c*-direction. The shape of the final graphite aggregate depends on the stacking of the platelets during their growth as foliated crystals and dendrites. While all aggregates start growing from the same nucleus, the tile-roof growth mode typical for lamellar graphite, produces graphite aggregates that appear to grow significantly in the *a*-direction, as stacking of the platelets is mostly along the *a*-axis.[13] With increased constitutional undercooling, as for compacted and

chunky graphite, stacking of the platelets is increasingly dominant along the *c*-axis, giving the appearance of growth in the *c*-direction. However, it is not the graphite crystal that grows in the *c*-direction, but the graphite aggregate. This growth mechanism does not require extensive growth of the graphite crystal in the *c*-direction by 2-D or spiral dislocation nucleation, nor by helical growth, and is supported by direct experimental observation presented in this work. Limited growth of the platelets in the *c*-direction is still required for the thickening of the platelets and the formation of blocky graphite.
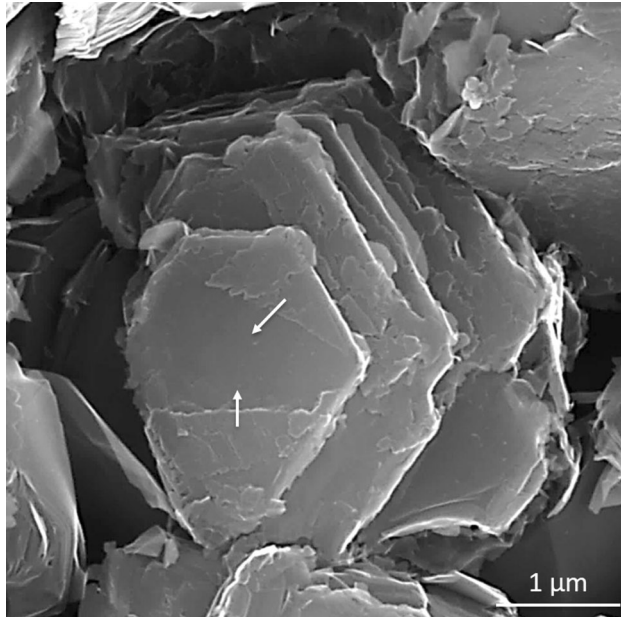
It is well known that impurities in the melt will affect the growth habitus of the graphite crystal. As recently suggested by Muhmond and Fredriksson[25] who used simulations with a molecule editor program, in the absence of defects, graphite crystals grow mainly in the *a*-direction. Because O and N in the melt can attach to the basal plane of the graphene layer, and because pentagonal, hexagonal, and high-order carbon-rings can be present as defects in the basal plane, growth along the *c*-direction, and/or curvature in the basal plane are favored. Other elements, such as S, Se, and B, attach to the basal plane and stabilize lamellar growth.

In spite of the progress in comprehending the crystallization of graphite from Fe-C melts, such facts as the impossibility to obtain well-rounded spheroidal graphite without Mg additions at typical industrial cooling rates of 0.5-10 K/s, require an answer before complete understanding can be reached.
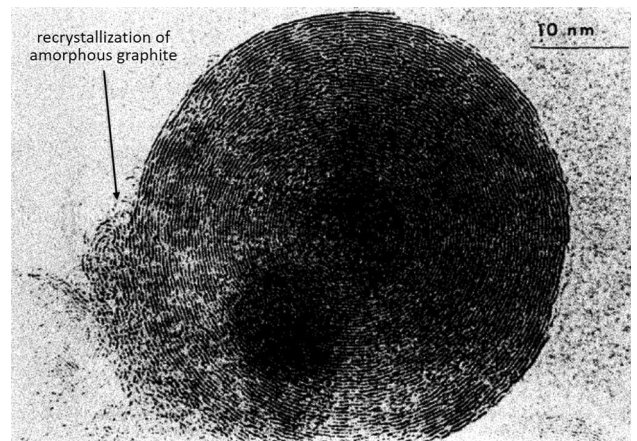

Fig. 17—Growth front of new graphene layers in a CG iron sample; arrows indicate the direction of growth.[13]

Fig. 19—High-resolution electron microscopy image of graphite spherulite formed by heating amorphous graphite in the electronic beam.[33]

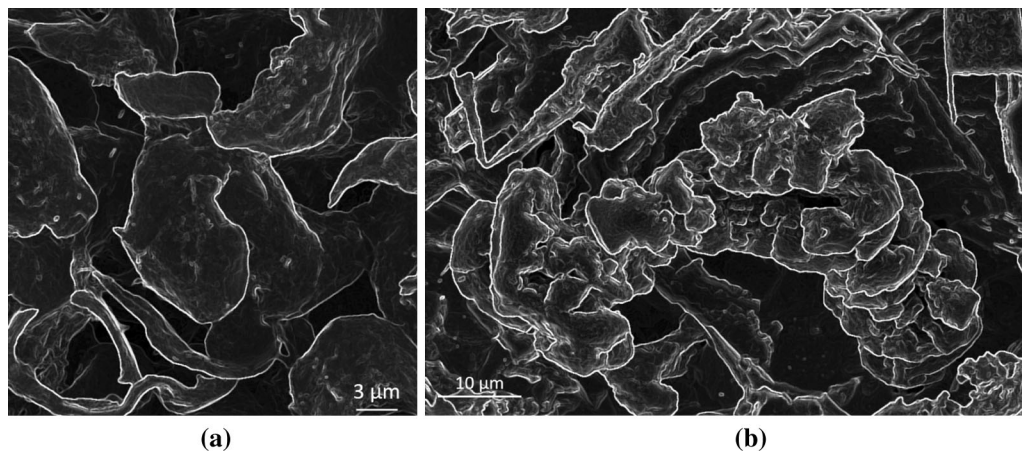(a)   (b)

Fig. 18—SEM micrograph of deep-etched samples: helical growth of graphite. (*a*) Early solidification (series CG-Q5); (*b*) sand cast (series CHG-S).
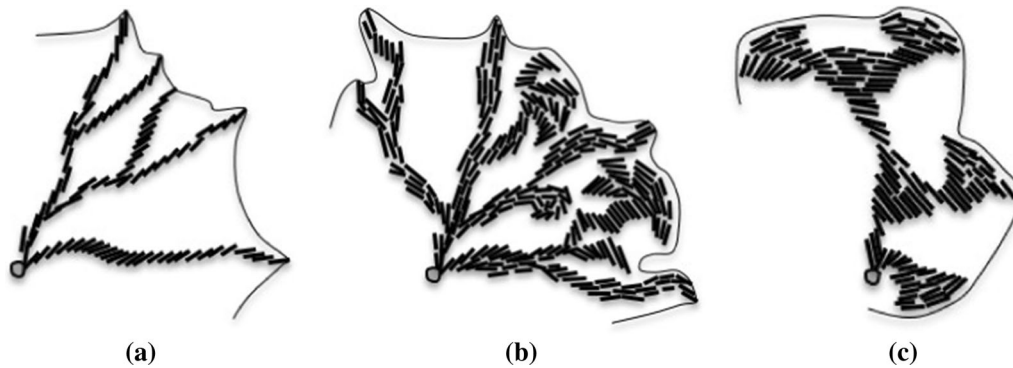
Fig. 20—Schematic representation of the mechanism of growth from the liquid for lamellar, compacted, and chunky graphite; short lines are the hexagonal graphite platelets. (*a*) Lamellar graphite; (*b*) compacted graphite; (*c*) chunky graphite.

IV. CONCLUSIONS

Extensive SEM work on interrupted solidification and sand-cooled cast iron specimens confirmed that compacted and chunky graphite grows radially from their respective nuclei as foliated crystals and dendrites. The building blocks of the graphite aggregates are hexagonal faceted graphite platelets, with nanometer height and micrometer width. Thickening of the platelets occurs through growth of additional graphene layers nucleated at the ledges of the graphite prism. Additional thickening, resulting in complete joining of the platelets, may occur from the recrystallization of the amorphous carbon that has diffused from the liquid through the austenite, once the graphite aggregate is enveloped in austenite. With increasing magnesium levels, the foliated graphite platelets acquire more disordered orientations and progressively aggregate along the *c*-axis forming clusters. The clusters that have random orientation eventually produce blocky graphite, as the spaces between the parallel platelets disappear through platelet thickening. This is typical for compacted graphite irons and tadpole graphite. Upon further increase in the magnesium content, the graphite platelets lose some of their hexagonal shape and begin organizing into graphite clusters stacked along the *c*-axis, producing the conical sectors typical for the chunky graphite aggregates. Sometimes helical growth appears to occur within the conical sectors. The large number of defects (cavities) observed in the graphite aggregates is consistent with growth of foliated crystals and dendrites.

REFERENCES

1. G.F. Geier, W. Bauer, B.J. McKay, and P. Schumacher: *Mater. Sci. Eng. A*, 2005, vols. 413–414, pp. 339–45.
2. D.K. Bandyopadhyay, D.M. Stefanescu, I. Minkoff and S.K. Biswal: *Physical Metallurgy of Cast Iron IV, Tokyo, Mat. Res. Soc. Proc.*, G. Ohira, T. Kusakawa and E. Niyama, eds., Pittsburgh, 1989, p. 27.
3. H. Itofuji and H. Uchikawa: *Trans. AFS*, 1990, vol. 98, pp. 429–48.
4. G. Alonso, D.M. Stefanescu, P. Larrañaga, and R. Suarez: *Int. J. Cast Metals Res.*, 2016, DOI:10.1179/1743133615Y.0000000020.
5. D.M. Stefanescu, G. Alonso, P. Larrañaga, and R. Suarez: *Acta Mater.*, 2016, vol. 103, pp. 103–14.
6. D.M. Stefanescu L. Dinescu, S. Craciun, M. Popescu, in Proc. 46th Int. Foundry Congress, CIATF Madrid, Spain, 1979, paper 37-1.
7. A. Velichko, C. Holzapfel, and F. Mücklich: *Adv. Eng. Mater.*, 2007, vol. 9, p. 39.
8. D.M. Stefanescu, F. Martinez, and I.G. Chen: *AFS Trans.*, 1983, vol. 91, pp. 205–16.
9. X.J. Deng, P.Y. Zhu, and Q.F. Liu: *AFS Trans.*, 1986, vol. 94, pp. 927–34.
10. S.I. Karsay and E. Compomanes: *AFS Trans.*, 1970, vol. 92, pp. 85–92.
11. P.C. Liu, C.L. Li, D.H. Wu, and C.R. Loper: *AFS Trans.*, 1983, vol. 91, pp. 119–26.
12. A.N. Roviglione and J.D. Hermida: *Metall. Mater. Trans. B*, 2004, vol. 35B, p. 313.
13. D.M. Stefanescu, G. Alonso, P. Larrañaga, E. De la Fuente, and R. Suarez: *Acta Mater.*, 2016, vol. 107, pp. 102–26.
14. D.D. Saratovkin: *Dendritic Crystallization*, Consultants Bureau, New York, 1959.
15. J. Sertucha, J. Lacaze, S. Armendariz, and P. Larrañaga: *Metall. Mater. Trans. A*, 2013, vol. 44A, pp. 1159–62, DOI:10.1007/s11661-012-1592-8.
16. H. Itofuji and A. Masutani: *Int. J. Cast Metals Res.*, 2001, vol. 14, pp. 1–14.
17. D.D. Double, and A. Hellawell: *The Metallurgy of Cast Iron*, B. Lux, I. Minkoff, and F. Mollard, eds., Georgi Publishing Co., St Saphorin, 1975, pp. 509–28.
18. S.H. Yoon, S. Lim, S.H. Hong, W. Qiao, D.D. Whitehurst, I. Mochida *et al.*: *Carbon*, 2005, vol. 43, pp. 1828–38.
19. D.D. Double and A. Hellawell: *Acta Metall. Mater.*, 1995, vol. 43, pp. 2435–42.
20. D.D. Double and A. Hellawell: *Acta Metall.*, 1969, vol. 17, pp. 1071–83.
21. D.H. St. John and L.M. Hogan: *J. Crystal Growth*, 1979, vol. 46, pp. 387–98.
22. M.C. Flemings: *Solidification Processing, McGraw Hill Series in Materials Science and Engineering*, McGraw Hill, New York, 1974.

23. W. Bollman, and B. Lux B: *The Metallurgy of Cast Iron*, B. Lux, I. Minkoff, F. Mollard, eds., Georgi Publishing, St. Saphorin, 1975, pp. 462–70.
24. E. Moumeni, N.S. Tiedje, A. Horsewell, J.H Hattel: A TEM Study on the Microstructure of Fine Flaky Graphite, *52nd International Foundry Conference*, Portoroz, Slovenia, 2012.
25. H.M. Muhmond and H. Fredriksson: *Metall. Mater. Trans. A*, 2014, vol. 45A, pp. 6187–99.
26. K. Theuwissen, J. Lacaze, and L. Laffont: *Carbon*, 2015, DOI:10.1016/j.carbon.2015.10.066.
27. S. Amini and R. Abbaschian: *Carbon*, 2013, vol. 51, pp. 110–23.
28. K.M. Fang, G.C. Wang, X. Wang, L. Huang, and G.D. Deng: in *Science and Processing of Cast Iron VIII*, Y.X. Li, H.F. Shen, Q.G. Xu, Z.Q. Han, eds., Tsinghua Univ. Press, Beijing, 2006, pp. 181–87.
29. I. Minkoff, I. Einbinder, Official Exchange Paper—Israel, International Foundry Congress, 1963, pp 139–43.
30. I. Minkoff: in *The Physical Metallurgy of Cast Iron, Stockholm, Mat. Res. Soc. Symposia Proc.*, H. Fredriksson, and M. Hillert, eds., North-Holland, 1985, pp. 37–45.
31. M. Hamasumi: *Trans. JIM*, 1965, vol. 6, pp. 234–39.
32. G.R. Purdy and M. Audier:Electron microscopical observations of graphite in cast irons in *The Physical Metallurgy of Cast Iron, Stockholm*, H. Fredriksson and M. Hillert, eds., Mat. Res. Soc. Symposia Proc, North-Holland, 1985, pp. 13–23.
33. D. Ugarte: *Nature*, 1992, vol. 359, p. 707.
34. J.P. Sadocha and J.E. Gruzleski:The mechanism of graphite spheroid formation in pure Fe-C-Si alloys in *The Metallurgy of Cast Iron*, B. Lux, I. Minkoff, and F. Mollard, eds., Georgi Publishing Co., St Saphorin, 1975, pp. 443–59.